

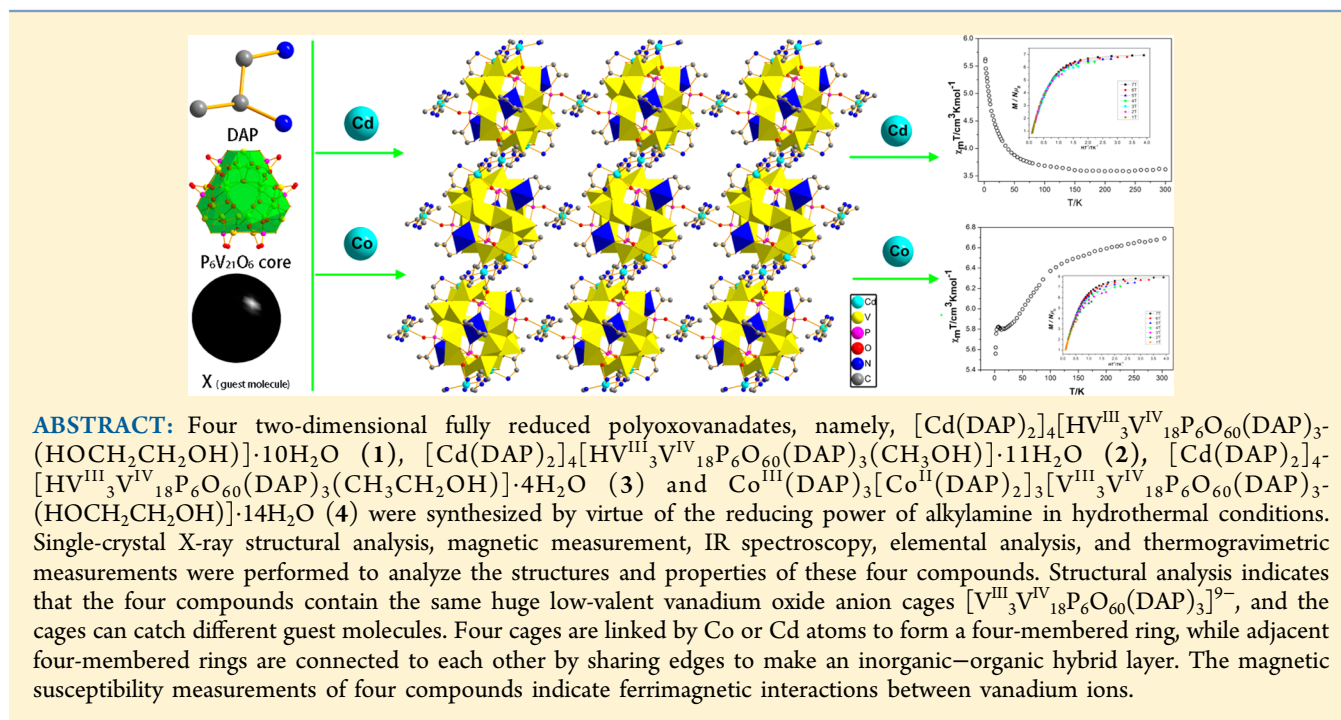
Four 2D “Fully Reduced” Polyoxovanadates: Vanadium Oxide Clusters Encapsulating Different Guest Molecules

Hongxiang Wan,[†] Congling Wang,[†] Yu Zhang,[†] Hao Miao,[†] Shuai Zhou,[†] and Yan Xu^{*,†,‡}

[†]College of Chemistry and Chemical Engineering, State Key Laboratory of Materials-Oriented Chemical Engineering, Nanjing Tech University, Nanjing 210009, P. R. China

[‡]Coordination Chemistry Institute, State Key Laboratory of Coordination Chemistry, Nanjing University, Nanjing 210093, P. R. China

S Supporting Information



INTRODUCTION

Polyoxometalates (POMs) are currently receiving considerable attention due to their aesthetically appealing structures and manifold applications. Compared with polyoxomolybdates and polyoxotungstates,^{1–8} polyoxovanadates as a prominent subclass of POMs are relatively less investigated. Vanadium ions exist in three oxidation states, namely, V(III), V(IV), and V(V), of which V(IV) atoms adopt four, five, or six-coordinated modes to form tetrahedral, square pyramidal, or octahedral coordination mode.⁹ Some polyoxovanadate clusters with Keggin $[\text{XV}_{12}\text{O}_{40}]^{n-}$ (X = heteroatom), the Wells–Dawson $[\text{X}_2\text{V}_{18}\text{O}_{62}]^{n-}$, and the Lindqvist structure $[\text{V}_6\text{O}_{19}]^{n-}$ have been reported.¹⁰ In the past few years, one important advance in vanadate chemistry has been studied of highly reduced polyoxovanadates as magnetic materials due to the large zero-field splitting (ZFS) of V(III) ion. More and more scholars are attracted to design and synthesize highly reduced V–O clusters with different structures, to explore their magnetic properties.^{11,12} One of the strategies used in the synthesis of highly

reduced V–O clusters materials is to employ a specific organic molecule or anion as the ligand of V atoms. In our previous work, when 1,2-diaminocyclohexane (DACH) was chosen as ligand to coordinate V(III) ions, a one-dimensional highly reduced polyoxovanadate constructed from low-valent vanadium cluster anions, $[\text{V}^{\text{III}}_3\text{V}^{\text{IV}}_{18}\text{P}_6\text{O}_{60}(\text{DACH})_3]^{9-}$, was obtained.¹³ Here, when we used a mixture of alcohol and water as solvent and chose 1,2-diaminopropane (DAP) as ligand, four two-dimensional (2D) highly reduced polyoxovanadates, namely, $[\text{Cd}(\text{DAP})_2]_4[\text{HV}^{\text{III}}_3\text{V}^{\text{IV}}_{18}\text{P}_6\text{O}_{60}(\text{DAP})_3(\text{HOCH}_2\text{CH}_2\text{OH})] \cdot 10\text{H}_2\text{O}$ (**1**), $[\text{Cd}(\text{DAP})_2]_4[\text{HV}^{\text{III}}_3\text{V}^{\text{IV}}_{18}\text{P}_6\text{O}_{60}(\text{DAP})_3(\text{CH}_3\text{OH})] \cdot 11\text{H}_2\text{O}$ (**2**), $[\text{Cd}(\text{DAP})_2]_4[\text{HV}^{\text{III}}_3\text{V}^{\text{IV}}_{18}\text{P}_6\text{O}_{60}(\text{DAP})_3(\text{CH}_3\text{CH}_2\text{OH})] \cdot 4\text{H}_2\text{O}$ (**3**), $\text{Co}^{\text{III}}(\text{DAP})_3[\text{Co}^{\text{II}}(\text{DAP})_2]_3[\text{V}^{\text{III}}_3\text{V}^{\text{IV}}_{18}\text{P}_6\text{O}_{60}(\text{DAP})_3(\text{HOCH}_2\text{CH}_2\text{OH})] \cdot 14\text{H}_2\text{O}$ (**4**) were successfully obtained. Structural analysis indicates the four compounds contain the

Received: July 2, 2014

Published: September 19, 2014

Table 1. Crystal Data and Structure Refinements for Four Compounds

compound	1	2	3	4
formula	Cd ₄ V ₂₁ P ₆ N ₂₂ C ₃₅ O ₇₂ H ₁₃₇	Cd ₄ V ₂₁ P ₆ N ₂₂ C ₃₄ O ₇₂ H ₁₃₇	Cd ₄ V ₂₁ P ₆ N ₂₂ C ₃₅ O ₆₅ H ₁₂₅	Co ₄ V ₂₁ P ₆ N ₂₄ C ₃₈ O ₇₆ H ₁₅₄
fw	3723.83	3711.82	3599.73	3655.13
T (K)	153(2)	153(2)	153(2) K	153(2) K
wavelength (Å)	0.710 73	0.710 73	0.710 73	0.710 73
cryst syst	monoclinic	monoclinic	monoclinic	monoclinic
space group	C2/c	C2/c	C2/c	P2 ₁ /c
a (Å)	16.174(3)	16.1652(16)	16.000(9)	16.212(2)
b (Å)	32.471(6)	32.456(3)	32.15(2)	33.124(4)
c (Å)	26.337(5)	26.362(3)	26.208(14)	25.237(3)
α (deg)	90	90	90	90
β (deg)	98.958(2)	98.9630(10)	98.974(7)	98.782(2)
γ (deg)	90	90	90	90
V (Å ³)	13663(4)	13662(2)	13315(13)	13394(3)
Z	4	4	4	4
D _c (g/cm ⁻³)	1.810	1.805	1.796	1.813
μ (mm ⁻¹)	2.127	2.126	2.175	2.036
F(000)	7368	7344	7096	7356
cryst size (mm ³)	0.16 × 0.14 × 0.14	0.16 × 0.13 × 0.12	0.16 × 0.13 × 0.12	0.15 × 0.14 × 0.13
limiting indices	-18 ≤ h ≤ 19, -38 ≤ k ≤ 38, -30 ≤ l ≤ 31	-19 ≤ h ≤ 19, -38 ≤ k ≤ 23, -31 ≤ l ≤ 31	-19 ≤ h ≤ 17, -38 ≤ k ≤ 29, -31 ≤ l ≤ 31	-19 ≤ h ≤ 18, -38 ≤ k ≤ 39, -30 ≤ l ≤ 30
θ range (deg)	1.25–25.00	1.25–25.02	1.27–25.02	1.02–25.02
reflns collected	48 015	38 133	40 767	88 887
indep reflns	12 048	12 078	11 541	23 570
R (int)	0.0395	0.0327	0.1067	0.0741
data/restraints/parameters	12 048/130/773	12 078/151/769	11 541/168/728	23 570/297/1548
GOF	1.180	1.150	1.097	1.134
R1 ^a , wR2 ^b [I > 2σ(I)]	0.0596, 0.1933	0.0605, 0.1997	0.0976, 0.2742	0.0755, 0.2321
R1, wR2 (all data)	0.0810, 0.2080	0.0796, 0.2147	0.1617, 0.3038	0.1165, 0.2555

^aR1 = $\sum ||F_o| - |F_c|| / \sum |F_o|$. ^bwR2 = $\sum [w(F_o^2 - F_c^2)^2] / \sum [w(F_o^2)^2]^{1/2}$.

largest highly reduced V–P–O cages, while the guest organic molecules are caught by [V^{III}₃V^{IV}₁₈P₆O₆₀(DAP)₃]⁹⁻ cages. The magnetic studies indicate these four compounds exhibit the presence of significant ZFS and interesting ferrimagnetic interactions.

EXPERIMENTAL SECTION

Materials and Physical Measurements. All chemicals were purchased from commercial sources and used without further purification. Powder X-ray diffraction (PXRD) were obtained on a Bruker D8X diffractometer equipped with monochromatized Cu Kα (λ = 1.5418 Å) radiation at room temperature. Data were collected in the range of 5–50°, and the experimental XRD patterns are in agreement with the patterns simulated on the basis of the single-crystal structures. The elemental analyses were performed on a PerkinElmer 2400 element analyzer. The infrared (IR) spectra were recorded on a Nicolet Impact 410 FTIR spectrometer using KBr pellets in the 4000–500 cm⁻¹ region. C, H, and N elemental analyses were performed on a PerkinElmer 2400 CHN elemental analyzer. Thermogravimetric analyses (TGAs) were carried out in N₂ atmosphere on a Diamond thermogravimetric analyzer from 25 to 800 °C with a heating rate of 10 °C/min. Magnetic susceptibility measurement of compounds were performed on a Quantum Design MPMS SQUID magnetometer using single-crystal samples at temperatures ranging from 2 to 300 K. The direct current measurements were collected using applied fields in the range of 0–7 T. The alternating current (AC) measurements were used to analyze a possible frequency dependence of the real and imaginary part of the magnetic susceptibility with amplitudes of 5 Oe in the frequency range from 1 to 1488 Hz. Data were corrected for contributions for the sample holder and for the diamagnetism according to the Pascal constants.

X-ray Crystallography. Data for the compounds of 1–4 were collected by using a Bruker Apex 2 CCD single-crystal diffractometer with Mo Kα radiation (λ = 0.710 73 Å) at 153 K using ω-2θ scan method. The single crystals of all compounds 1–4 were chosen and held on a thin glass fiber by epoxy glue in air for data collection. The SHELX software package (Bruker) was used to solve and refine the structures. Absorption corrections were applied empirically using the SADABS program. All the non-hydrogen atoms were refined anisotropically. The hydrogen atoms of organic molecule were placed in calculated positions, assigned isotropic thermal parameters, and allowed to ride on their parent atoms, while the H atoms of water and disordered organic molecules were not located. All calculations were performed using the SHELX97 program package. Further details of the X-ray structural analyses for compounds 1–4 are given in Table 1.

Synthesis of [Cd(DAP)₂]₄[HV^{III}₃V^{IV}₁₈P₆O₆₀(DAP)₃(HOCH₂CH₂OH)]·10H₂O (1). A mixture of V₂O₅ (0.3000 g, 1.65 mmol), Cd(CH₃COO)₂·4H₂O (0.1337 g, 0.5 mmol), DAP (0.5 mL), H₂O (5 mL), H₃PO₄ (50 wt %, 0.1241 g, 0.633 mmol), and ethylene glycol (2 mL) was stirred 30 min in air. The mixture was then transferred to a 25 mL Teflon-lined autoclave and heated to 170 °C for 5 d. After the mixture cooled to room temperature, dark block crystals were obtained by filtration, washed with distilled water, and dried in air. Yield 0.25 g, 43.2% (based on V). Elemental analysis calcd (%) for C₃₅H₁₃₇N₂₂O₇₂P₆V₂₁Cd₄: C 11.32, N 8.03, H 3.81, V 28.86, Cd 12.13; found: C 11.28, N 8.28, H 3.68, V 28.73, Cd 12.07. IR of compound 1 (cm⁻¹): 3450 s, 2920 s, 1630 s, 1460 vs, 1382 vs, 1170 vs, 1068 s, 993 s, 877 s, 684 w.

Synthesis of [Cd(DAP)₂]₄[HV^{III}₃V^{IV}₁₈P₆O₆₀(DAP)₃(CH₃OH)]·11H₂O (2). A mixture of V₂O₅ (0.3000 g, 1.65 mmol), Cd(CH₃COO)₂·4H₂O (0.1337 g, 0.5 mmol), DAP (0.5 mL), H₂O (5 mL), H₃PO₄ (50 wt %, 0.1241 g, 0.633 mmol), and methyl alcohol (2 mL) was stirred 30 min in air. The mixture was then transferred to a 25 mL Teflon-lined autoclave and heated to 170 °C for 5 d. After the mixture cooled

to room temperature, dark block crystals were obtained by filtration, washed with distilled water, and dried in air. Yield 0.23 g, 39.7% (based on V). Elemental analysis calcd (%) for $C_{34}H_{137}N_{22}O_{72}P_6V_{21}Cd_4$: C 11.36, N 8.39, H 3.65, V 28.86, Cd 12.18; found: C 11.00, N 8.30, H 3.72, V 28.82, Cd 12.11. IR of compound **2** (cm^{-1}): 3432 s, 2933 s, 1585 vs, 1452 vs, 1380 vs, 1159 s, 1074 s, 892 s, 692 s.

Synthesis of $[Cd(DAP)_2]_4[HV^{III}_3V^{IV}_{18}P_6O_{60}(DAP)_3(CH_3CH_2OH)] \cdot 4H_2O$ (3**).** A mixture of V_2O_5 (0.3000 g, 1.65 mmol), Cd- $(CH_3COO)_2 \cdot 4H_2O$ (0.1337 g, 0.5 mmol), DAP (0.5 mL), H_2O (5 mL), H_3PO_4 (50 wt %, 0.1241 g, 0.633 mmol), and ethanol (2 mL) was stirred 30 min in air. The mixture was then transferred to a 25 mL Teflon-lined autoclave and heated to 170 °C for 5 d. After the mixture cooled to room temperature, dark block crystals were obtained by filtration, washed with distilled water, and dried in air. Yield 0.25 g, 43.2% (based on V). Elemental analysis calcd (%) for $C_{35}H_{125}N_{22}O_{65}P_6V_{21}Cd_4$: C 11.86, N 8.19, H 3.65, V 29.86, Cd 12.74; found: C 11.68, N 8.56, H 3.50, V 29.72, Cd 12.49. IR of compound **3** (cm^{-1}): 3419 s, 2971 s, 1596 w, 1382 vs, 1066 vs, 944 vs, 678 s.

Synthesis of $Co^{III}(DAP)_3[Co^{II}(DAP)_2]_3[V^{III}_3V^{IV}_{18}P_6O_{60}(DAP)_3 \cdot (HOCH_2CH_2OH)] \cdot 14H_2O$ (4**).** A mixture of V_2O_5 (0.3000 g, 1.65 mmol), $Co(CH_3COO)_2 \cdot 4H_2O$ (0.1284 g, 0.5 mmol), DAP (0.5 mL), H_2O (5 mL), H_3PO_4 (50 wt %, 0.1241 g, 0.633 mmol), and ethylene glycol (2 mL) was stirred 30 min in air. The mixture was then transferred to a 25 mL Teflon-lined autoclave and heated to 170 °C for 5 d. After the mixture cooled to room temperature, dark block crystals were obtained by filtration, washed with distilled water, and dried in air. Yield 0.24 g, 41.8% (based on V). Elemental analysis calcd (%) for $C_{38}H_{154}N_{24}O_{76}P_6V_{21}Co_4$: C 12.63, N 9.41, H 4.35, V 29.53, Co 6.52; found: C 12.54, N 9.24, H 4.23, V 29.40, Co 6.48. IR of compound **4** (cm^{-1}): 3434 s, 2920 s, 1632 w, 1383 vs, 1077 vs, 986 vs, 882 s, 678 s, 576 s.

RESULTS AND DISCUSSION

Synthesis Discussion. Although products always contain many impurities, solvothermal synthesis is also a powerful method in the synthesis of polyoxovanadates. As we all know, sometimes imperceptible changes in solvent, pH value, stirring time, the type of initial reactants, and reaction temperature and time can change the nucleation and growth of final products. In our case, organic amine (DPA) plays important roles, not only as a reducing agent but also coordinating to V(III) ions in the final products. We found that changing the ratio of solvent and reaction temperature resulted in lower yield of final four products. In addition, according to our experiments, the four compounds have good reproducibility.

Crystal Structures of (1), (2), and (3). The experimental and simulated XRD patterns of four compounds are displayed in Supporting Information, Figure S9. The experimental peak positions of four compounds accord well with the simulated XRD pattern, which shows the phase purity of four compounds. X-ray structural analysis reveals that compounds **1**, **2**, and **3** are composed of cluster anions $[HV^{III}_3V^{IV}_{18}P_6O_{60}(DAP)_3(X)]^{8-}$ ($X =$ ethylene glycol, methyl alcohol, or ethanol), $\{[Cd(DAP)_2]_4\}^{8+}$ cations, and water molecules. Take compound **1** as an example. Since the nanosized anion $[HV^{III}_3V^{IV}_{18}P_6O_{60}(DAP)_3(HOCH_2CH_2OH)]^{8-}$ has C3 axis and lies on a symmetry plane ($2 - x, y, 0.5 - z$), compound **1** is racemic mixture. As shown in Figure 1, nanosized anion of **1** consists of 18 VO_5 square pyramids, three $[VO_4(DAP)_3]^{5-}$ scaffolding vanadyl moieties, and six PO_4^{3-} groups (Supporting Information, Figure S1). There are two types of five-coordinated vanadium in the polyanion of **1** (Supporting Information, Figure S2a,b). One, the basal position of square-pyramidal geometry, is defined by the oxygen donors from each of the two adjacent phosphate groups, two μ_3 oxygen groups, and the apical position by the terminal oxide group; another,

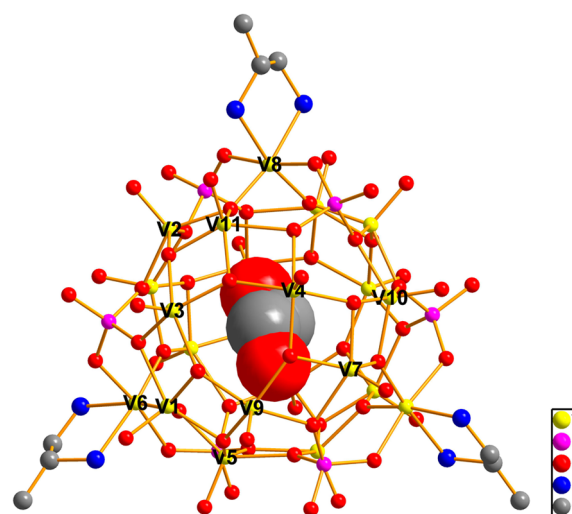


Figure 1. Representative view of the central polyoxovanadate core $[HV^{III}_3V^{IV}_{18}P_6O_{60}(DAP)_3(HOCH_2CH_2OH)]^{8-}$ in **1**.

the basal position of square-pyramidal geometry, is defined by the oxygen donors from each of the one adjacent phosphate group, three μ_3 oxygen groups, and the apical position by the terminal oxide group. The 18 five-coordinated vanadium atoms (V1, V2, V3, V4, V5, V7, V9, V10, V11, and their crystallographic partners) adopt a distorted square pyramidal configuration, with a short axial vanadyl bond [1.595(4)–1.622(3) Å] and four equatorial bonds in the range of 1.912(3)–2.069(4) Å. The bond valence sum (BVS) calculation¹⁴ indicates the oxidation states of above V atoms are +4, while V–O bond distances are comparable with V(IV) compounds.^{15,16} In the structure of $[HV^{III}_3V^{IV}_{18}P_6O_{60}(DAP)_3 \cdot (HOCH_2CH_2OH)]^{8-}$, two crown-type $[V_6O_{18}]$ units are connected by three $[V_2O_8]$ short spiral chains to form a V_{18} cage. One $[VO_4N_2]$ regular octahedron and two PO_4 tetrahedra are sharing corners to make a handlelike $[VP_2O_{10}N_2(DPA)]$ moiety. Three $[VP_2O_{10}N_2(DPA)]$ groups are attached to V_{18} cage to generate an interesting $[HV^{III}_3V^{IV}_{18}P_6O_{60}(DAP)_3(HOCH_2CH_2OH)]^{8-}$ inorganic–organic hybrid cage. Both V6 and V8 atoms in $[VP_2O_{10}N_2(DPA)]$ group exhibit an octahedral geometry, and each V atom is coordinated by four O from two adjacent V–O polyhedra, two PO_4 tetrahedra, and two N atoms from a bidentate DAP ligand (Supporting Information, Figure S2). The V–O and V–N bond distances are 1.919(3)–2.036(3) and 2.151(5)–2.160(5) Å, respectively, which are comparable with V–O(N) bond lengths in the reported V(III) compounds.^{16,7–9} Application of the BVS calculation¹⁴ suggests both V6 and V8 are in the oxidation state of +3.¹⁷ The tetrahedral P–O bond distances are in the range of 1.472(4)–1.585(3) Å, with the O atom with the longest P–O bond coordinating to the vanadium center, which is similar to those reported vanadates.^{15,16} More interestingly, an ethylene glycol molecule is encapsulated in the large $[HV^{III}_3V^{IV}_{18}P_6O_{60}(DAP)_3]^{8-}$ anions in **1**. To the best of our knowledge, low-valent vanadate cages that have caught guest molecules are very rare,¹⁷ while $[HV^{III}_3V^{IV}_{18}P_6O_{60}(DAP)_3 \cdot (HOCH_2CH_2OH)]^{8-}$ is the first fully reduced low-valent vanadium oxide cage anion known to have caught a guest molecule. Ethylene glycol molecule in the center of the cage adapts symmetry plan by using disorder, as shown in Supporting Information, Figure S3.

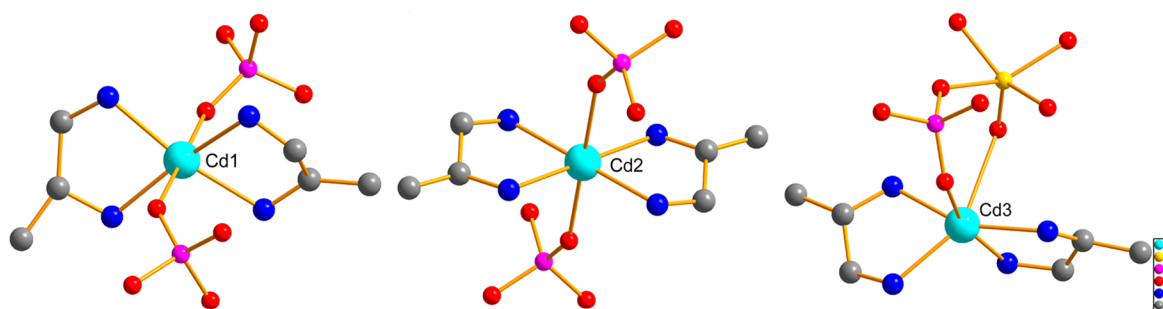


Figure 2. View of different coordination environments around the Cd atoms.

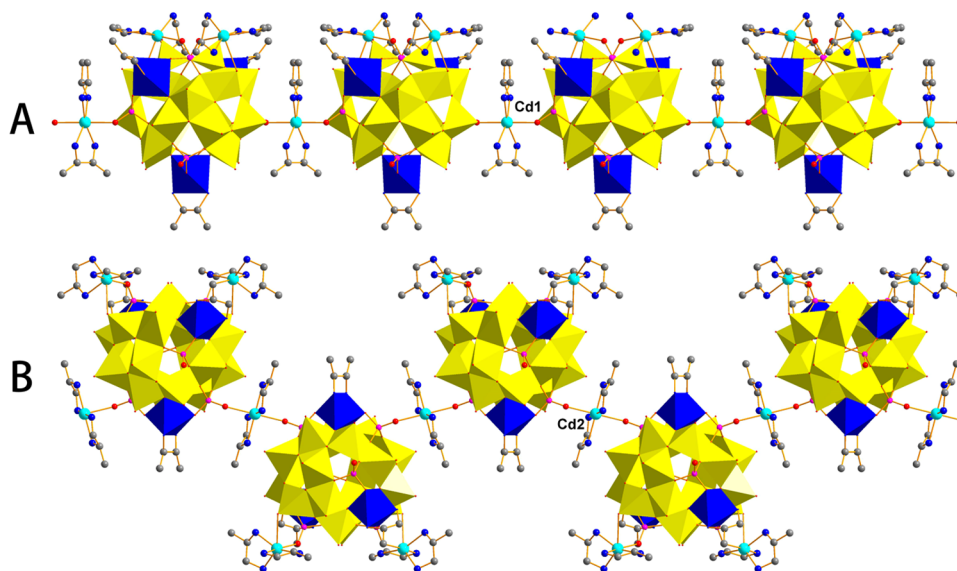


Figure 3. Two types chains in 1.

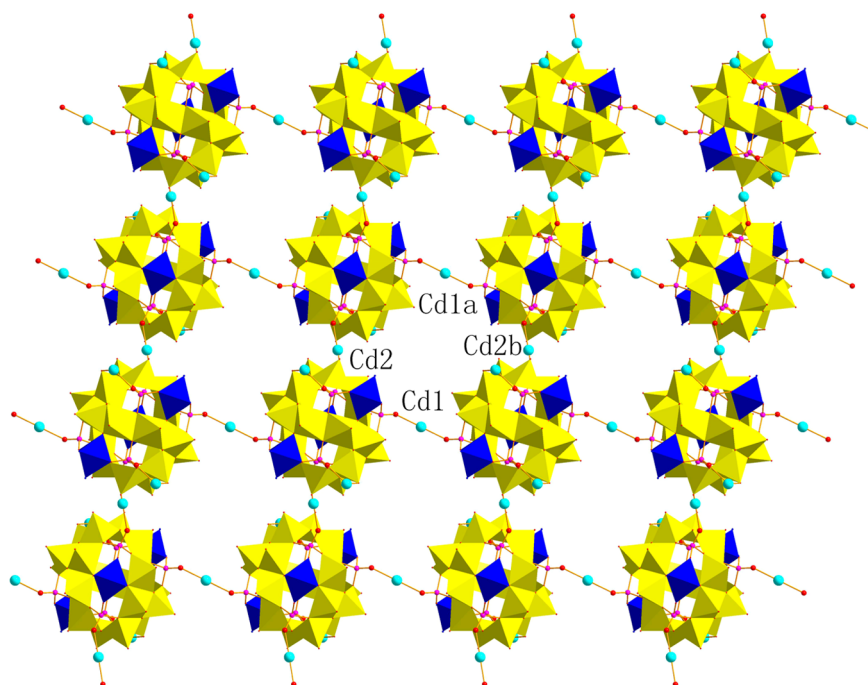


Figure 4. 2D layer of the compound 1. Symmetry codes: a: $3 - x, -y, -z$; b: $1 + x, y, z$.

There are three crystallographic independent Cd ions in 1. As shown in Figure 2, the Cd1 and Cd2 atoms exhibit a

distorted octahedron coordinated by four nitrogen atoms of two DPA molecules, and two oxygen atoms of PO_4^{3-} from two

neighboring clusters. There are two types of chains in **2**. As shown in Figure 3, Cd1 connects two adjacent $[\text{HV}^{\text{III}}_3\text{V}^{\text{IV}}_{18}\text{P}_6\text{O}_{60}(\text{DAP})_3(\text{HOCH}_2\text{CH}_2\text{OH})]^{8-}$ anions to make a linear-type $\{[\text{HV}^{\text{III}}_3\text{V}^{\text{IV}}_{18}\text{P}_6\text{O}_{60}(\text{DAP})_3(\text{HOCH}_2\text{CH}_2\text{OH})]^{-}\text{Cd}(\text{DAP})_2\}_n$ chain (A), while Cd2 links two neighboring clusters to form a zigzag $\{[\text{HV}^{\text{III}}_3\text{V}^{\text{IV}}_{18}\text{P}_6\text{O}_{60}(\text{DAP})_3(\text{HOCH}_2\text{CH}_2\text{OH})]^{-}\text{Cd}(\text{DAP})_2\}_n$ chain (B). Both types of chains are connected each other to get a novel $\{[\text{HV}^{\text{III}}_3\text{V}^{\text{IV}}_{18}\text{P}_6\text{O}_{60}(\text{DAP})_3(\text{HOCH}_2\text{CH}_2\text{OH})]^{-}\text{Cd}(\text{DAP})_2\}_n$ layer, which is the first example of layered fully reduced vanadium compound, as shown in Figure 4. Cd3 atom is five-coordinated by four nitrogen atoms of two DPA molecules and one oxygen atom of PO_4^{3-} . CdN_4O trigonal bipyramid (Cd3) is attached in the surface of V–O–P–Cd layer. The bond distances of Cd–O and Cd–N are 2.316(3)–2.397(3) Å and 2.252(5)–2.330(6) Å, respectively. If we regard the clusters as nodes, the nodes are connected by Cd to form a wavelike 2D grid structure. The blue nodes represent Cd atoms, and the black nodes represent $[\text{HV}^{\text{III}}_3\text{V}^{\text{IV}}_{18}\text{P}_6\text{O}_{60}(\text{DAP})_3(\text{X})]^{8-}$ clusters (see Figure 5). Water molecules are

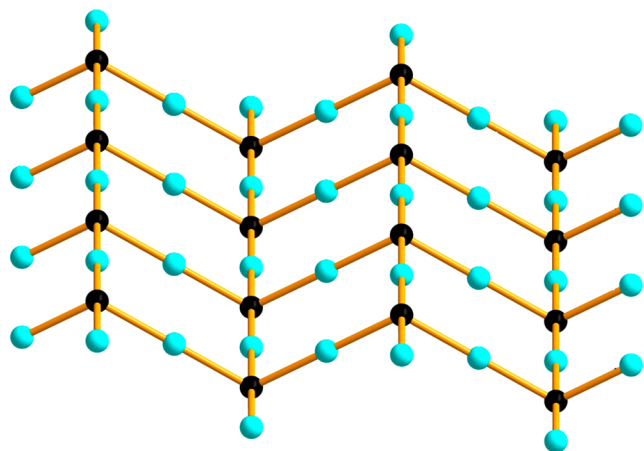


Figure 5. Topology net of compound **1**.

inserted between layers and involved hydrogen bonding interactions with adjacent layers to generate a three-dimensional (3D) supramolecular structure (see Supporting Information, Figure S6). The various hydrogen bonds are listed in Supporting Information, Table S2. Compounds **2** and **3** keep the same topological structure, only different guest molecules are caught by $[\text{HV}^{\text{III}}_3\text{V}^{\text{IV}}_{18}\text{P}_6\text{O}_{60}(\text{DAP})_3]^{8-}$ cage (see Supporting Information, Figure S4).

Crystal Structures of (4). Similar to **1**, compound **4** is constructed by cage anions $[\text{V}^{\text{III}}_3\text{V}^{\text{IV}}_{18}\text{P}_6\text{O}_{60}(\text{DAP})_3\text{HOCH}_2\text{CH}_2\text{OH}]^{9-}$, $\{[\text{Co}^{\text{II}}(\text{DAP})_2]_3\}^{6+}$ cations,

$[\text{Co}^{\text{III}}(\text{DAP})_3]^{3+}$ cations, and water molecules. There are four crystallographically independent Co ions in **1**. As shown in Figure 6, Co3 and Co4 are six-coordinated by four N atoms and two O atoms from $[\text{V}^{\text{III}}_3\text{V}^{\text{IV}}_{18}\text{P}_6\text{O}_{60}(\text{DAP})_3(\text{HOCH}_2\text{CH}_2\text{OH})]^{9-}$ cages. Co3, Co4, Co3a, and Co4a link four cages to form a ring of $[\text{V}^{\text{III}}_3\text{V}^{\text{IV}}_{18}\text{P}_6\text{O}_{60}(\text{DAP})_3(\text{HOCH}_2\text{CH}_2\text{OH})]_4[\text{Co}(\text{DAP})_2]_4$, as shown in Figure 7. Adjacent rings are connected to each other by sharing edges

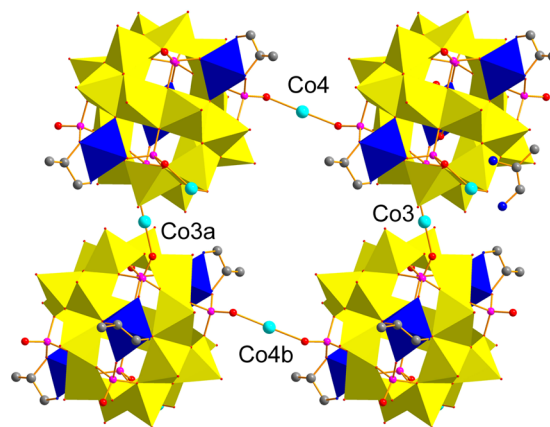


Figure 7. Ring formed by cages and Co atoms in **4**. Symmetry codes: a: $-1 + x, y, z$; b: $x, 1.5 - y, 0.5 + z$.

to make an inorganic–organic hybrid layer. Co1 is coordinated by six N atoms from three DAP ligands to get an isolated coordination cation of $[\text{Co}^{\text{III}}(\text{DAP})_3]^{3+}$, which is located at the center of $[\text{V}^{\text{III}}_3\text{V}^{\text{IV}}_{18}\text{P}_6\text{O}_{60}(\text{DAP})_3(\text{HOCH}_2\text{CH}_2\text{OH})]_4[\text{Co}(\text{DAP})_2]_4$ ring. Co2 is five-coordinated by four nitrogen atoms of two DPA molecules and one oxygen atom of PO_4^{3-} . CoN_4O tetragonal pyramids (Co2) are attached in the surface of V–O–P–Co layer (Figure 8). Charge considerations require the presence of three Co(II) atoms and one Co(III) atom, and based on bond distances, Co1 is in the +3 oxidation state (all bond distances are in the 1.942(5)–1.991(4) Å range), while Co2, Co3, and Co4 are assigned to the +2 oxidation state (bond distances in the 2.066(7)–2.264(3) Å range).¹⁸ Also, water molecules link adjacent layers to generate a 3D supramolecular by using hydrogen bonds. Compared with our previous work, the steric hindrance of DAP is much smaller than that of DACH; four novel 2D coordination polymers constructed by nanosized fully reduced $[\text{V}^{\text{III}}_3\text{V}^{\text{IV}}_{18}\text{P}_6\text{O}_{60}(\text{DAP})_3(\text{X})]^{8-}$ cages were obtained.

Magnetic Property. Given the large magnetic anisotropy of V^{III} ions with a $3d^2$ electronic configuration, the variable-temperature magnetic properties of four compounds were measured on an MPMS SQUID VSM magnetometer in the

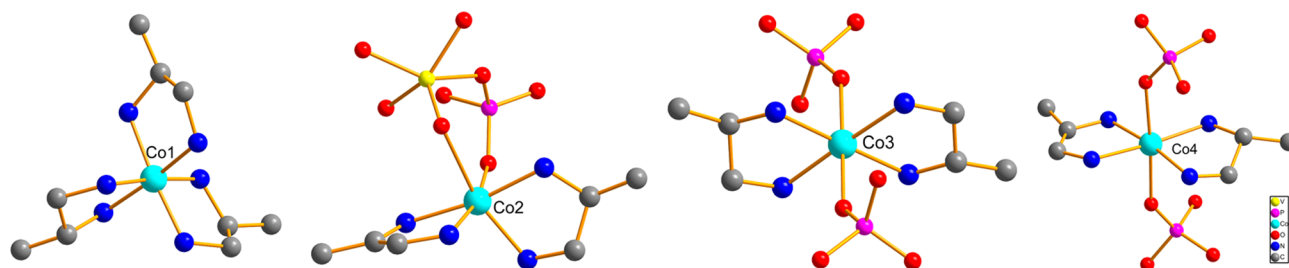


Figure 6. View of different coordination environments around the Co atoms.

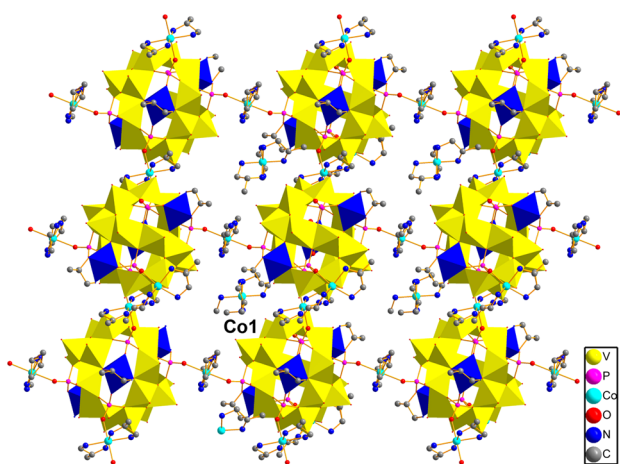


Figure 8. 2D structure of the compound 4.

field of 2 kOe and the range from 300 to 2 K. Because the Cd^{2+} complexes are diamagnetic, the $\chi_{\text{M}}T$ products of 1, 2, and 3 are almost dependent upon the polyoxovanadate anions. As shown in Figure 9, the $\chi_{\text{M}}T$ values of compounds 1, 2, and 3 are $4.346 \text{ cm}^3 \text{ K mol}^{-1}$, $4.938 \text{ cm}^3 \text{ K mol}^{-1}$, and $4.753 \text{ cm}^3 \text{ K mol}^{-1}$ at room temperature, which are smaller than the expected value ($9.75 \text{ cm}^3 \text{ K mol}^{-1}$) for total uncoupled $18 \text{ V}^{4+} (S = 1/2)$ and 3

$\text{V}^{3+} (S = 1)$ ions. As the system cooled, the $\chi_{\text{M}}T$ products first gradually decreased, and then $\chi_{\text{M}}T$ products increased to the maximum values of $6.83 \text{ cm}^3 \text{ K mol}^{-1}$, $8.13 \text{ cm}^3 \text{ K mol}^{-1}$, and $7.84 \text{ cm}^3 \text{ K mol}^{-1}$.

The $\chi_{\text{M}}T$ product of 4 is dependent upon the Co^{2+} and the polyoxovanadate anions. As shown in Figure 9, the $\chi_{\text{M}}T$ value of compound 4 is $6.69 \text{ cm}^3 \text{ K mol}^{-1}$ at room temperature, which is smaller than the expected value ($15.38 \text{ cm}^3 \text{ K mol}^{-1}$) for total uncoupled $18 \text{ V}^{4+} (S = 1/2)$, $3 \text{ V}^{3+} (S = 1)$, and $\text{Co}^{2+} (S = 3/2)$ ions. As the system cooled, the $\chi_{\text{M}}T$ product first gradually decreased, and then $\chi_{\text{M}}T$ product increased to the value of $5.82 \text{ cm}^3 \text{ K mol}^{-1}$.

The four shapes of the curve show a ferrimagnet-like nature, indicating that the antiferromagnetic coupling between vanadium ions dominates the magnetic properties of four compounds, but the ground-state spin is not zero. Therefore, the very low $\chi_{\text{M}}T$ values at room temperature imply that the antiferromagnetic coupling exists in temperatures higher even than 300 K, and the experimental values of $\chi_{\text{M}}T$ may approach the Curie constant. As shown in Figure 10, the unsaturated magnetization values of $8.42 \text{ N}\mu_{\text{B}}$, $9.25 \text{ N}\mu_{\text{B}}$, $8.97 \text{ N}\mu_{\text{B}}$, and $7.96 \text{ N}\mu_{\text{B}}$ at 7 T further conform the antiferromagnetic coupling between metal ions in four compounds.

When the temperature dropped to a point, the $\chi_{\text{M}}T$ values of compounds 2, 3, and 4 dropped sharply, possibly because of the alignment of spins at metal ions saturated along the

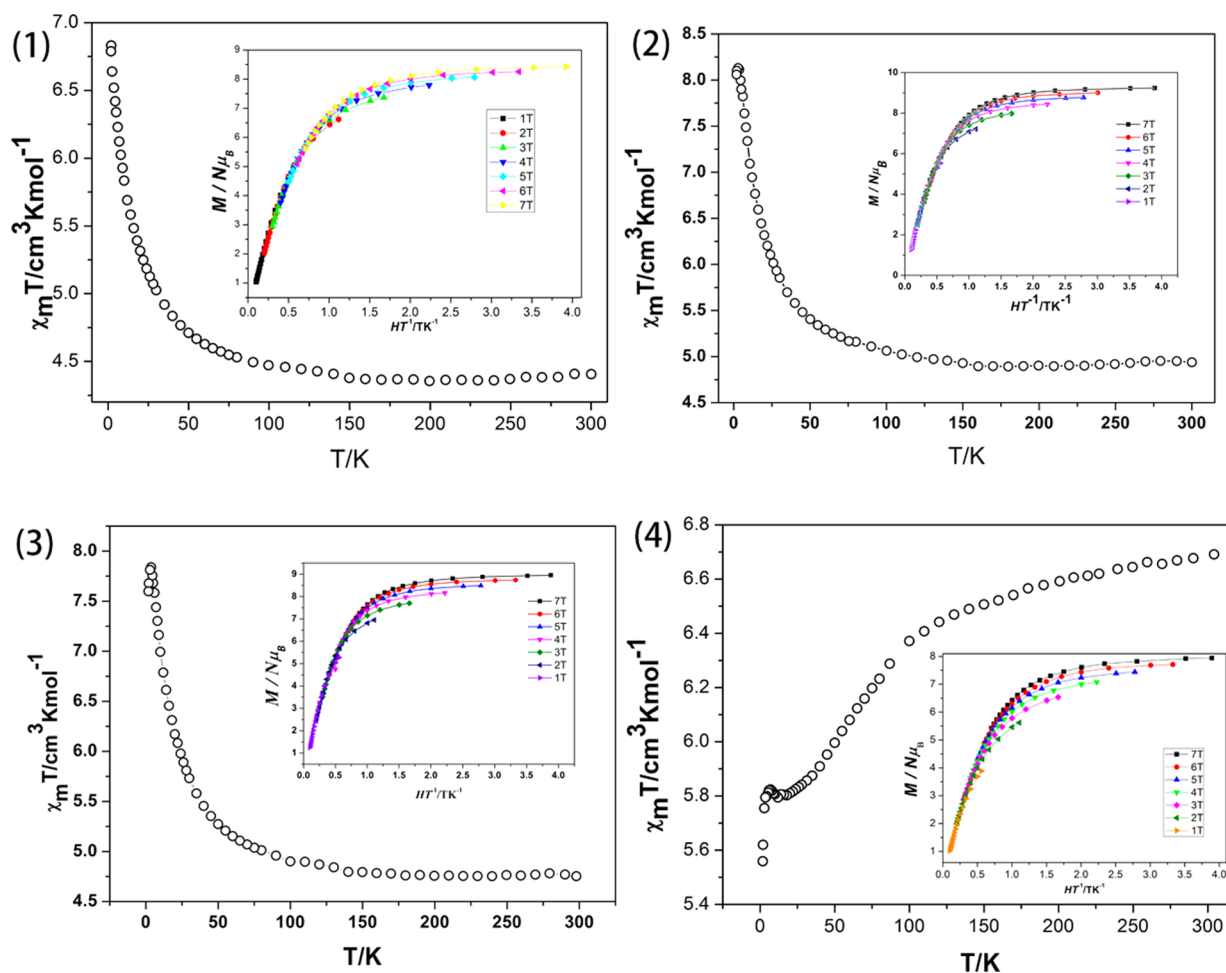


Figure 9. Temperature dependence of $\chi_{\text{M}}T$ for four compounds at 2 kOe. (inset) Reduced magnetization data for four compounds at low temperature.).

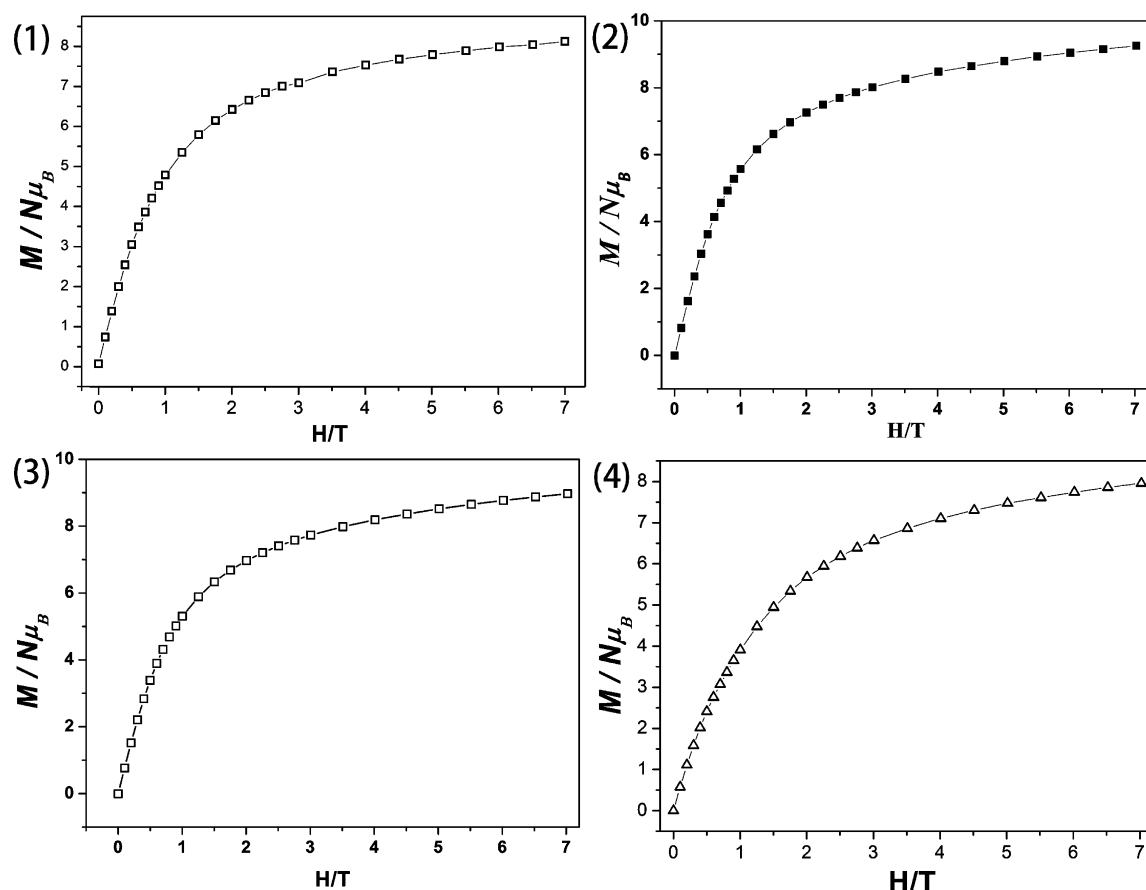


Figure 10. Field dependence of magnetization for four compounds measured at 1.8 K. (The lines are guides.)

direction of applied field, the presence of ZFS in the ground state, and the antiferromagnetic interaction between clusters. Since no signal was observed in the plot of out-of-phase AC susceptibilities (as shown in Supporting Information, Figure S7), compounds **1**, **2**, and **4** do not exhibit single-molecule magnet behavior.¹⁹

CONCLUSIONS

In conclusion, we have synthesized four 2D fully reduced polyoxovanadates by using DAP. The four compounds contain the same vanadium oxide cage $[\text{V}^{\text{III}}_3\text{V}^{\text{IV}}_{18}\text{P}_6\text{O}_{60}(\text{DACH})_3]^{9-}$ anions, and the cages can catch different guest molecules. Magnetic susceptibility measurement of four compounds indicates ferrimagnetic interactions between vanadium ions.

ASSOCIATED CONTENT

Supporting Information

Structural diagrams, plot of temperature variation of the in-phase and out-of-phase products for compounds **1**, **2**, and **4**, tables of data indicating BVS of compound **1** and H-bond interactions in four compounds, IR spectra, PXRD patterns, and TGA plotted data. This material is available free of charge via the Internet at <http://pubs.acs.org>.

AUTHOR INFORMATION

Corresponding Author

*E-mail: yanxu@njtech.edu.cn. Phone: 86-25-83587857. Fax: 86-25-83211563.

Notes

The authors declare no competing financial interest.

ACKNOWLEDGMENTS

We thank the Natural Science Foundation of Jiangsu Province, China (Grant No. BK2012823), and the Project of Priority Academic Program Development of Jiangsu Higher Education Institutions and Qing Lan Project.

REFERENCES

- (a) Mei, H.; Yan, D. W.; Chen, Q.; Xu, Y.; Sun, Q. *Inorg. Chim. Acta* **2010**, *363*, 2265–2268. (b) Yan, D. W.; Zheng, L.; Zhang, Z. B.; Wang, C. L.; Yuan, Y.; Zhu, D. R.; Xu, Y. *J. Coord. Chem.* **2010**, *63*, 4215–4225.
- (a) Yan, D. W.; Fu, J.; Zheng, L.; Zhang, Z. B.; Xu, Y.; Zhu, X. L.; Zhu, D. R. *CrystEngComm* **2011**, *13*, 5133–5141. (b) Yan, D. W.; Chen, Q.; Xu, Y.; Sun, Q.; Zhu, D. R.; Song, Y.; Elangovan, S. P. *Inorg. Chem. Commun.* **2011**, *14*, 1314–1317.
- (a) Fu, J.; Sun, H. X.; Xu, Y.; Wang, C. L.; Zhu, D. R.; Sun, Q.; Liu, H. K. *CrystEngComm* **2012**, *14*, 5148–5150. (b) Guo, J. Y.; Jin, X. F.; Chen, L.; Wang, Z. X.; Xu, Y. *J. Coord. Chem.* **2012**, *65*, 3821–3832.
- (a) Xu, X.; Yan, D. W.; Fan, X. R.; Xu, Y. *J. Coord. Chem.* **2012**, *65*, 3674–3683. (b) Xu, X.; Ju, W. W.; Hou, W. T.; Zhu, D. R.; Xu, Y. *CrystEngComm* **2014**, *16*, 82–88.
- (a) Xu, X.; Ju, W. W.; Yan, D. W.; Jian, N. G.; Xu, Y. *J. Coord. Chem.* **2013**, *66*, 2669–2678. (b) Lin, B. Z.; Chen, Y. M.; Liu, P. D. *Dalton. Trans.* **2003**, 2474–2477.
- (a) Han, Z. H.; Zhao, Y. L.; Peng, J.; Ma, H. Y.; Liu, Q.; Wang, E. B.; Hu, N. H.; Jia, H. Q. *Eur. J. Inorg. Chem.* **2005**, 264–271. (b) Ren, Y. P.; Kong, X. J.; Hu, X. Y.; Sun, M.; Long, L. S.; Huang, R. B.; Zheng, L. S. *Inorg. Chem.* **2006**, *45*, 4016–4023.
- (a) Nogueira, H. I. S.; Paz, F. A. A.; Teixeira, P. A. F.; Kilinowskib, J. *Chem. Commun.* **2006**, 2953–2955. (b) Sha, J.; Peng, J.;

Lan, Y.; Su, Z.; Pang, H.; Tian, A.; Zhang, P.; Zhu, M. *Inorg. Chem.* **2008**, *47*, 5145–5153.

(8) Liu, H.; Qin, C.; Wei, Y. G.; Xu, L.; Gao, G. G.; Li, F. Y.; Qu, X. S. *Inorg. Chem.* **2008**, *47*, 4166–4172.

(9) Diego, S. I.; Jared, S. S.; Vojtech, J.; Christopher, C. C. *Inorg. Chem.* **2011**, *50*, 9980–9984.

(10) (a) Sun, C. Y.; Liu, S. X.; Liang, D. D.; Shao, K. Z.; Ren, Y. H.; Su, Z. M. *J. Am. Chem. Soc.* **2009**, *131*, 1883–1888. (b) Li, S. J.; Liu, S. M.; Liu, S. X.; Liu, Y. W.; Tang, Q.; Shi, Z.; Ouyang, S. X.; Ye, J. H. *J. Am. Chem. Soc.* **2012**, *134*, 19716–19721. (c) Che, M.; Fournier, M.; Launay, J. P. *J. Chem. Phys.* **1979**, *71*, 1954–1960.

(11) (a) Gatteschi, D.; Caneschi, A.; Pardi, L.; Sessoli, R. *Science* **1994**, *265*, 1054–1058. (b) Clemente-Juan, J. M.; Coronado, E.; Gdel, H.; Mutka, H. *Chem.—Eur. J.* **2002**, *8*, 5701–5708. (c) Calzado, C. J.; Clemente-Juan, J. M.; Coronado, E.; Suaud, N. *Inorg. Chem.* **2008**, *47*, 5889–5901.

(12) (a) Sadakane, M.; Steckhan, E. *Chem. Rev.* **1998**, *98*, 219–237. (b) Daniel, C.; Hartl, H. J. *Am. Chem. Soc.* **2005**, *127*, 13978–13987. (c) Tidmarsh, I. S.; Scales, E.; Brearley, P. R.; Laye, R. H.; McInnes, E. J. L. *Inorg. Chem.* **2007**, *46*, 9743–9753. (d) Kortz, U.; Müller, A.; Slageren, J.; Schnack, J.; Dalal, N. S.; Dressel, M. *Coord. Chem. Rev.* **2009**, *253*, 2315–2327.

(13) Wang, C. L.; Zhang, Z. B.; Fu, J.; Xu, Y.; Zhu, D. R. *Chem.—Eur. J.* **2012**, *18*, 11909–11912.

(14) Brown, I. D. *Chem. Rev.* **2009**, *109*, 6858–6919.

(15) (a) Laye, R. H.; Wei, Q.; Mason, P. V.; Shanmugam, M.; McInnes, E. J. L. *J. Am. Chem. Soc.* **2006**, *128*, 9020–9021. (b) Tidmarsh, I. S.; Laye, R. H.; Shanmugam, M.; McInnes, E. J. L. *Chem.—Eur. J.* **2007**, *13*, 6329–6338. (c) Aronica, C.; Chastanet, G.; Zueva, E.; Borshch, S. A.; Luneau, D. *J. Am. Chem. Soc.* **2008**, *130*, 2365–2371.

(16) (a) Gatteschi, D.; Pardi, L.; Barra, A.-L.; Müller, A.; Doring, J. *Nature* **1991**, *354*, 463–465. (b) Kortz, U.; Müller, A.; Slageren, J.; Schnack, J.; Dalal, N. S.; Dressel, M. *Coord. Chem. Rev.* **2009**, *253*, 2315–2327. (c) Khanra, S.; Kloth, M.; Mansaray, H.; McInnes, E. J. L.; Winpenny, R. E. P. *Angew. Chem., Int. Ed.* **2007**, *46*, 5568–5571.

(17) (a) Müller, A.; Sessoli, R.; Krickemeyer, E.; Bolgge, H.; Meyer, J.; Gatteschi, D.; Pardi, L.; Westphal, J.; Hovemeier, K.; Rohlfing, R.; Doring, J.; Hellweg, F.; Beugholt, C.; Schmidtmann, M. *Inorg. Chem.* **1997**, *36*, 5239–5250. (b) Keene, T. D.; D'Alessandro, T. D.; Kramer, T. D.; Price, J. R.; Price, D. J.; Decurtins, S.; Kepert, C. J. *Inorg. Chem.* **2012**, *51*, 9192–9199.

(18) (a) Angelos, B. C.; Demetrios, I. T.; Aggelos, P.; George, E. K.; Constantinos, J. M. *Inorg. Chem.* **2012**, *51*, 10461–10470. (b) Qin, C.; Xu, L.; Wei, Y.; Wang, X.; Li, F. *Inorg. Chem.* **2003**, *42*, 3107–3110.

(19) (a) Sessoli, R.; Gatteschi, D.; Caneschi, A.; Novak, M. A. *Nature* **1993**, *365*, 141–143. (b) Laye, R. H.; McInnes, E. J. L. *Eur. J. Inorg. Chem.* **2004**, 2811–2818. (c) Proust, A.; Thouvenot, R.; Gouzerh, P. *Chem. Commun.* **2008**, *16*, 1837–1852.